LBL-18623 c.2

Lawrence Berkeley Laboratory

UNIVERSITY OF CALIFORNIA

RECEIVED
LAWRENCE
BERKELEY LABORATORY
198
Y AND

Materials & Molecular Research Division

Presented at the Science of Hard Materials 2nd International Conference, Rhodes, Greece, September 21-28, 1984

MICROSTRUCTURE, MECHANICAL PROPERTIES AND WEAR OF Fe-3Cr-0.4C STEELS

Y.S. Yoon and G. Thomas

August 1984

TWO-WEEK LOAN COPY
This is a Library Circulating Copy which may be borrowed for two weeks.

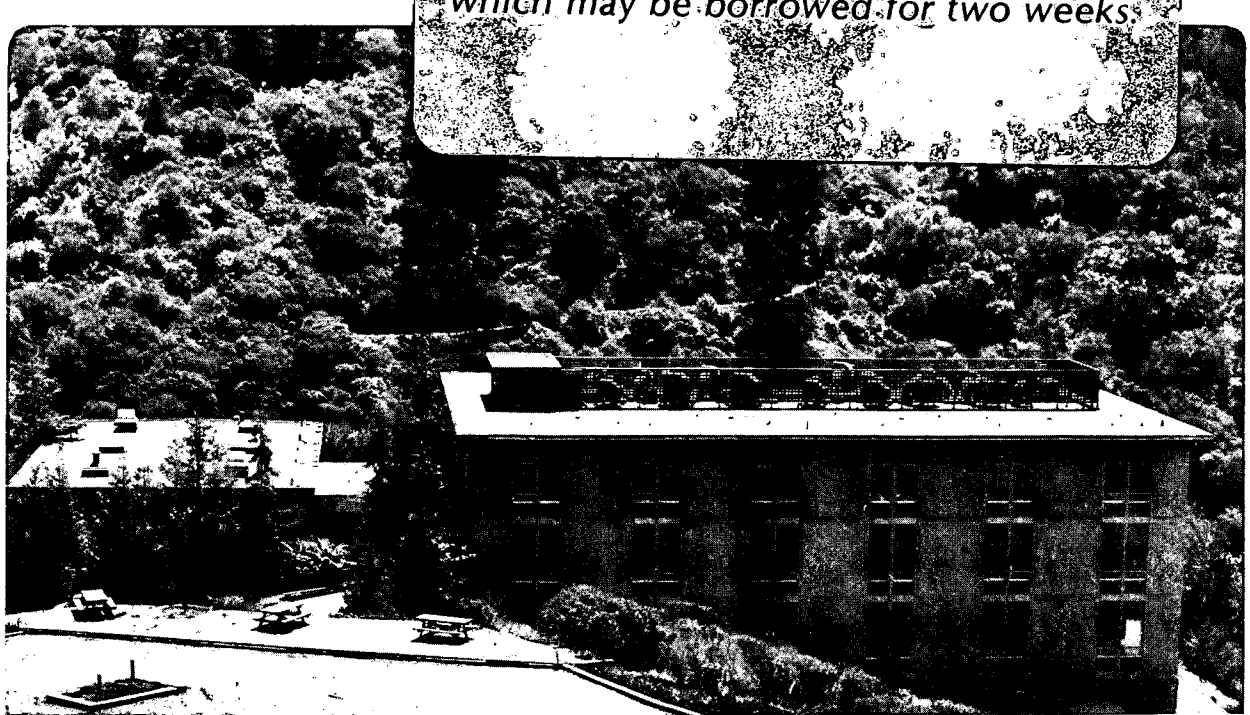

Prepared for the U.S. Department of Energy under Contract DE-AC03-76SF00098

LBL-18623 c.2

DISCLAIMER

This document was prepared as an account of work sponsored by the United States Government. While this document is believed to contain correct information, neither the United States Government nor any agency thereof, nor the Regents of the University of California, nor any of their employees, makes any warranty, express or implied, or assumes any legal responsibility for the accuracy, completeness, or usefulness of any information, apparatus, product, or process disclosed, or represents that its use would not infringe privately owned rights. Reference herein to any specific commercial product, process, or service by its trade name, trademark, manufacturer, or otherwise, does not necessarily constitute or imply its endorsement, recommendation, or favoring by the United States Government or any agency thereof, or the Regents of the University of California. The views and opinions of authors expressed herein do not necessarily state or reflect those of the United States Government or any agency thereof or the Regents of the University of California.

MICROSTRUCTURE, MECHANICAL PROPERTIES AND WEAR OF FE-3CR-0.4C STEELS

Y. S. YOON, AND G. THOMAS

Department of Materials Science and Mineral Engineering and Materials and Molecular Research Division, Lawrence Berkeley Laboratory, University of California, Berkeley, California, 94720

ABSTRACT

The structure-property relationships of an ultra-high strength steel with a chemical composition that was based on Fe-3Cr-0.4C are described. The microstructure, which consisted of dislocated lath martensite containing fine carbides and interlath thin films of retained austenite, was found to give combinations of mechanical properties and abrasion-resistance that are attractive in comparison to many commercial abrasive alloys. It is also shown that thermo-mechanical treatments can improve both toughness and abrasion resistance by attaining a fine grain size with finely dispersed alloy carbides, when microalloying additions (Mo,V) are present.

INTRODUCTION

Ultra-high strength steels are mainly used in aircraft landing gear, rocket motor cases, missiles bodies, bearings and shafts, armour plate, and other defense applications [1]. Since such steels have high hardness and consequently high abrasion resistance, they are also used in mining and mineral processing equipment such as buckets, chutes and loader shovels. Recently, the recognition of coal as an important source of energy has brought more significance to such steels.

Over the last decade, systematic investigations of the effect of alloying elements on the structure and the mechanical properties of martensite have led to the development of an optimum composition of Fe/3Cr/2Mn/0.5Mo/0.3C [2]. The microstructure of this alloy is characterized by dislocated lath martensite surrounded by interlath films of retained austenite [Fig. 1] and results in superior combinations of strength and toughness over many commercial alloys.

The martensite transformation in steels is perhaps the most exploited transformation to produce a variety of strength and toughness combinations at high strength levels. If controlled so that the inhomogeneous shear component occurs by slip rather than by twinning, the martensite transformation is the most efficient method of producing a high density of dislocations, uniformily distributed in a fine-grained microstructure [3]. The dislocations are necessary for both strength and toughness. The main factor controlling this aspect of the transformation is composition, especially carbon content, which must be regulated to maintain Ms> 300°C

[4]. In this study two changes were made in the composition of Fe/3Cr/2Mn/0.5Mo/0.3C in order to try to achieve good combinations of strength, toughness and wear resistance. The carbon content was raised to 0.4 wt. pct since the most common method of increasing the hardness and the strength of martensite is through raising the carbon content. The Mn content was correspondingly reduced to 1 wt. pct in order to maintain Ms >300°C and thus prevent the formation of twinned martensite which would be coupled with the increased carbon level. The principles of the alloy design approach used have been summarized in the previous conference [5]. Occasionally wear is compounded when parts are exposed to elevated temperatures. For instance, coal feeders that feed dry coal pellets into a pressure vessel are exposed to temperatures of the order of 500°C [6]. Plain carbon or low alloy steels would normally lose hardness at these temperatures. To meet these industrial requirements, secondary hardening steels, that is, alloy steels containing strong carbide forming elements such as Mo and V, have long been used in certain manufacturing industries.

With secondary hardening steels, the austenitizing temperature must be sufficiently high to dissolve all carbides, otherwise poor toughness occurs [7]. However, austenite grains coarsen rapidly at these high temperatures, and this also lowers impact toughness. Consequently, simple austenitizing treatments at high temperatures cannot be applied to these steels, when it is necessary to improve the toughness.

From these points of view, thermal-mechanical treatments may be the most suitable for secondary hardening steels to obtain small prior austenite grains without undissolved carbides. Also, strain induced fine alloy carbide precipitation can be achieved during controlled rolling and can accelerate grain refining, as e.g., in ausforming. However, their effects on the mechanical properties, and abrasion resistance are not well known. Consequently, in this investigation controlled rolling has also been performed on a modified experimental steel (alloy B, Table 1), and the effects of strain induced fine scale alloy carbides on mechanical properties and abrasion resistance have been studied as a function of tempering temperature.

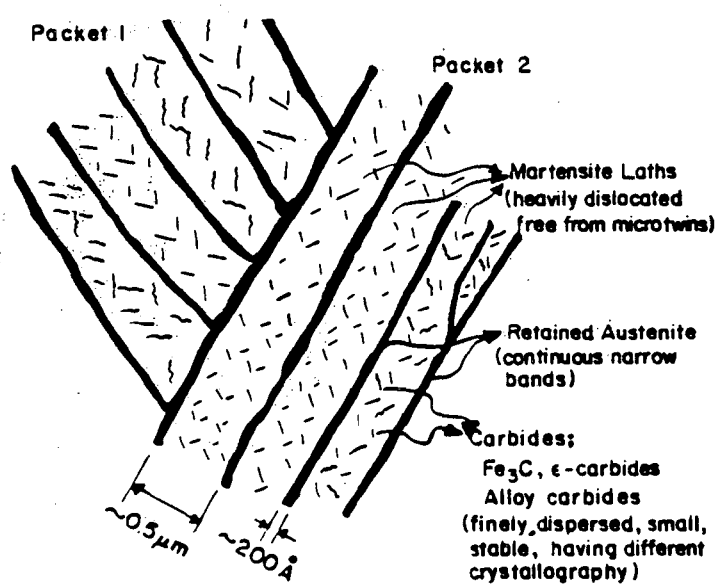

Fig. 1. Scheme showing desired composite microstructure of lath martensite and thin films of retained austenite to provide good combinations of high strength and toughness.

TABLE 1 Alloy Compositions and Transformation Temperatures

Alloy Design.	C	Cr	Mn	Mo	V	Si	Cu	P	S	Fe	Ms	Mf	As	Af
	Composition, Wt. Pct.										Meas. Temp. °C			
A	0.39	3.02	1.01	0.51	-	0.01	0.01	0.003	0.006	Bal.	310	200	780	820
B	0.41	3.01	0.99	0.51	1.01	0.04	0.02	0.003	0.005	Bal.	300	200	790	830

EXPERIMENTAL PROCEDURE

The nominal compositions of the alloys used in this investigation and the transformation temperature determined by dilatometric measurements are listed in Table 1. They were vacuum induction melted into 20 lb. ingots and subsequently rolled to 1 in. thick and 25 in. wide plates. The plates were homogenized under argon atmosphere at 1200°C for 24 hours and then furnace cooled. The heat treatment applied to alloy A in this investigation was austenitizing at 900°C for 1 hour, followed by quenching and tempering at various temperatures. The heat treatment and the controlled rolling process applied to alloy B are schematically illustrated in Fig. 2. The austenitizing treatments were carried out in a vertical tube furnace under an argon atmosphere. After austenitizing or controlled rolling the specimens were quenched into agitated oil. All the tempering treatments (200°C through 590°C) were carried out by immersing the specimens into a salt pot for 1 hour and then quenching into agitated oil. Tensile testing, Charpy testing and plane strain fracture toughness testing were conducted in accordance with the standard ASTM specifications. Rockwell C hardness testing was performed on the Charpy specimens. Two-body abrasive wear tests were conducted using a pin-on-disc tester which simulates high-stress abrasion [9]. Wear specimens for the test were obtained by machining broken Charpy bars. The wear pins were worn against abrasive paper for 10 revolutions at a rotational speed of 20 rpm under 1 kg deadweight load over a spiral track of 2.2 meters in length. The abrasive paper used was 120 grit SiC. A break-in run was carried out prior to each of the three wear tests performed on each pin. The subsequent weight losses were measured on a Metler balance, sensitive to 0.01 mg, and a mean value was calculated. The weight loss was then determined and converted to wear resistance as shown below:

$$\text{wear resistance} \quad \frac{(\text{material density}) \times (\text{length of wear path}) \ (\text{mm})}{\text{weight loss} \ (\text{mm}^3)} \qquad 1$$

Microstructural characterization was carried out using optical microscopy and transmission electron microscopy (TEM). Thin foils for TEM were obtained from broken Charpy specimens, and were examined in a Philips EM 301 microscope at an operating voltage of 100 kV. Energy dispersive X-Ray (EDX) analysis was conducted on carbon extraction replicas using a Philips EM 400 scanning-transmission electron microscope. Fractography was conducted on Charpy specimens, using an ISI scanning electron microscope.

RESULTS AND DISCUSSION

A. Microstructural Characterization

1) Optical Metallography

Optical metallography was carried out to observe any variations in the

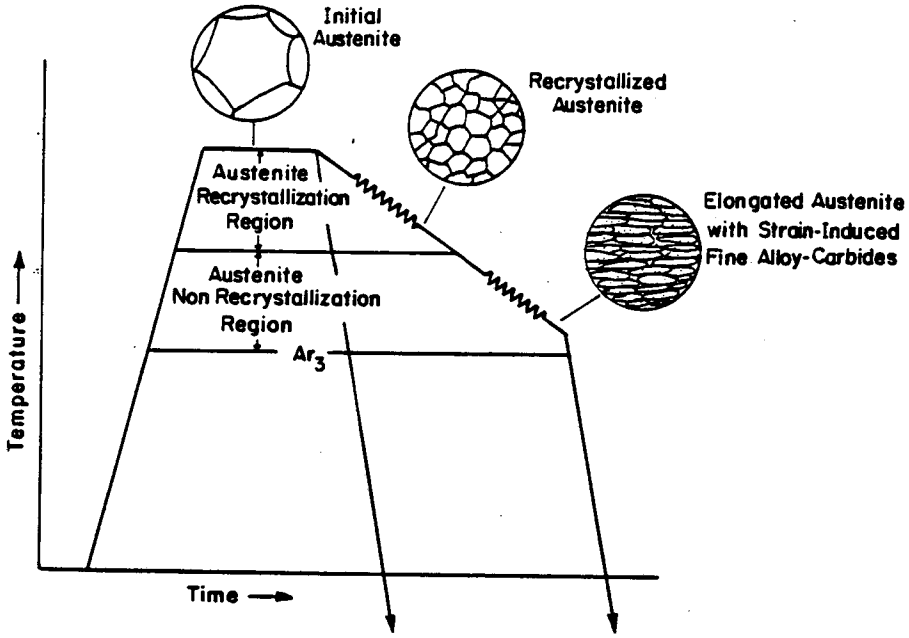

Fig 2. Schematic illustration of heat treatment and controlled rolling process applied to alloy B.

gross features of microstructure, e.g., prior austenite grain size, coarse undissolved carbides or inclusions, if present, and so forth. Fig. 3 shows the optical microstructure of alloy A, after being austenitized at 900°C for 1 hr. and then quenched. Fig. 3a shows a typical martensitic structure and Fig. 3b shows the prior austenite grain size to be ~35 μm.

Fig. 4 shows representative optical micrographs for alloy B austenitized at various temperatures, i.e., 1000°C(4a), 1100°C (4b), and 1200°C(4c). A large number of undissolved coarse carbides were observed in the structure austenitized at 1000°C. As the austenitizing temperature was increased, the number of undissolved carbides decreased yet they became coarser (Fig. 4b). After the austenitizing at 1200°C (Fig. 4c), the undissolved carbides could hardly be resolved optically. Fig. 5 shows representative optical micrographs for alloy B treated thermally or thermomechanically. The structure prior to rolling, obtained by quenching after solution treatment (1200°C, 1 hr.), is shown in Fig. 5a. It shows that the average size of the prior austenite grains is 500 μm. The large prior austenite grains were not recrystallized by the 50% reduction at 850°C (Fig. 5b). They were just elongated. However, rolling to a 50% reduction at 1150°C completely recrystallized the large prior austenite grains and reduced the average grain size to 40 μm (Fig. 5c). After two rolling passes of 50% reduction each at 1150°C and 850°C, the prior austenite grains were refined and elongated (Fig. 5d). From these micrographs, it is clear that a high temperature austenitizing treatment followed by controlled rolling is suitable for secondary hardening steels to obtain a fine grain structure without undissolved coarse carbides.

(ii) Transmission Electron Microscopy

Structural characterization by transmission electron microscopy was performed on the quenched and tempered structures.

(a) As-Quenched Structure

The martensite morphology of the alloys investigated in this study is basi-

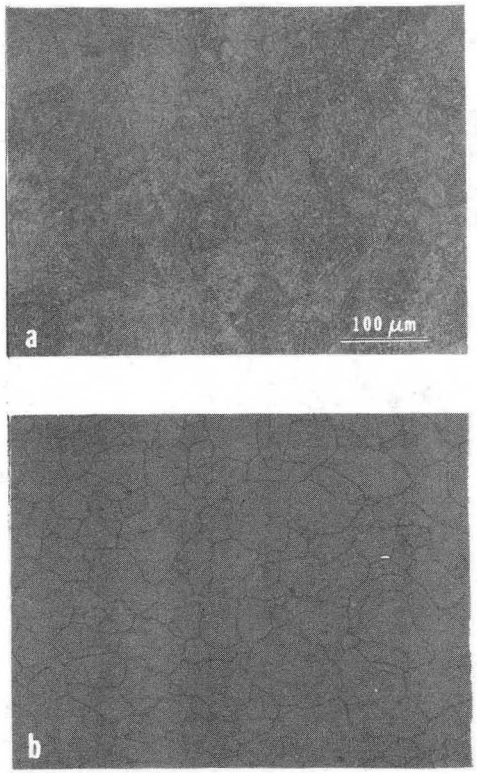

Fig 3. Optical micrographs of the as-quenched structure of alloy A. (a) shows the martensite structure and (b) shows the prior austenite grain boundaries.

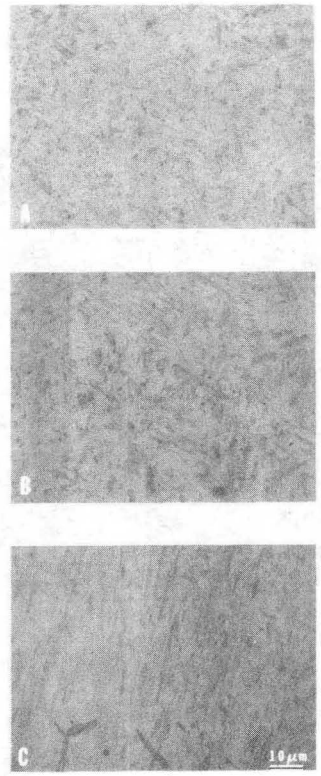

Fig 4. Optical micrographs of the as-quenched structures of alloy B austenitized at (a) 1000°C (b) 1100°C and (c) 1200°C.

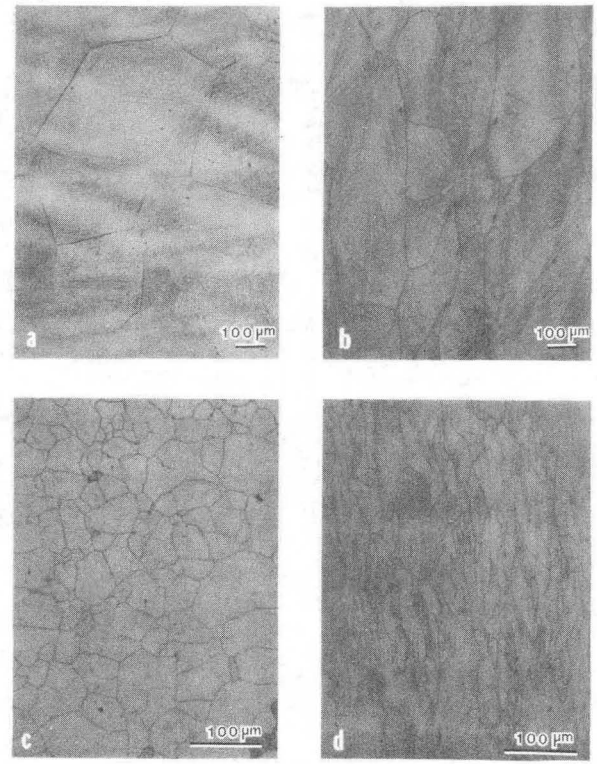

Fig 5. Optical micrographs of alloy B (a) austenitized at 1200°C for 1 hr., (b) austenitized at 1200°C for 1 hr., hot rolled o 50% reduction at 850°C (c) austenitized at 1200°C for 1 hr., hot rolled to 50% reduction at 1150°C, and (d) austenitized at 1200°C for 1 hr. hot rolled at 1150°C and 850°C by 50% reduction each.

cally a dislocated lath type (Figs. 6 and 7b), as desired by the design criteria [5]. However, a small amount of twinned martensite (about 10% of the observed structure) was observed in the microstructure of thermally treated alloy B (austenitized at 1200°C for 1 hr. and quenched, (Fig. 7a). These observations indicate that the addition of 1% V and the higher austenitizing temperature increased the tendency to form twinned plates. No twinned martensite was observed in the microstructure of the controlled rolled alloy B (rolled at 1150°C and 850°C by 50% reduction at each temperature (Fig. 7b) and the average width of the laths is about 0.1 μm. These fine laths may be a consequence of a reduced carbon level in the austenite caused by the strain-induced precipitation of fine vanadium carbides [5][Fig. 8].

The observed auto-tempered carbides in the microstructure of alloy A were identified as ε- carbides [Fig. 9]. It is not clear under what conditions ε-carbide forms or what morphology it has. However, ε-carbide is described as 'cross-hatched' [12,13] carbide because of its appearance in electron microscopy of thin foils. In the as-quenched or the low-temperature

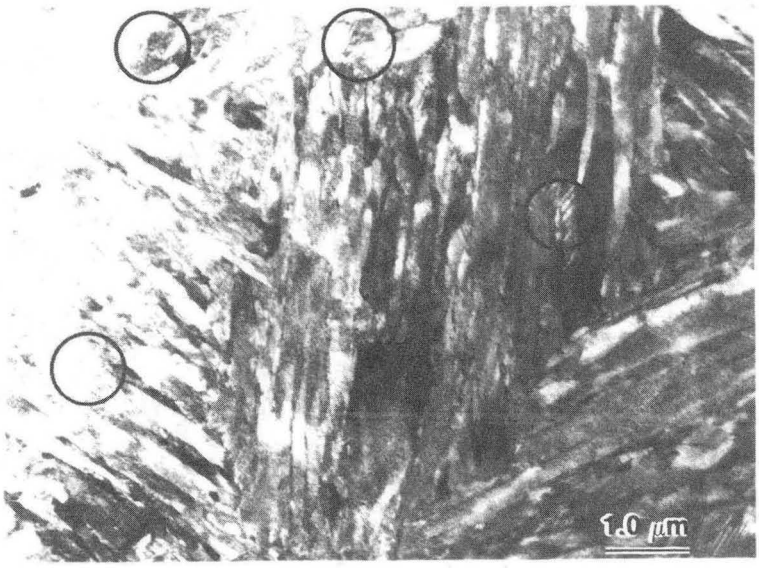

Fig 6. A bright field (BF) micrograph showing characteristic configuration of laths and packets in the as-quenched structure of alloy A.

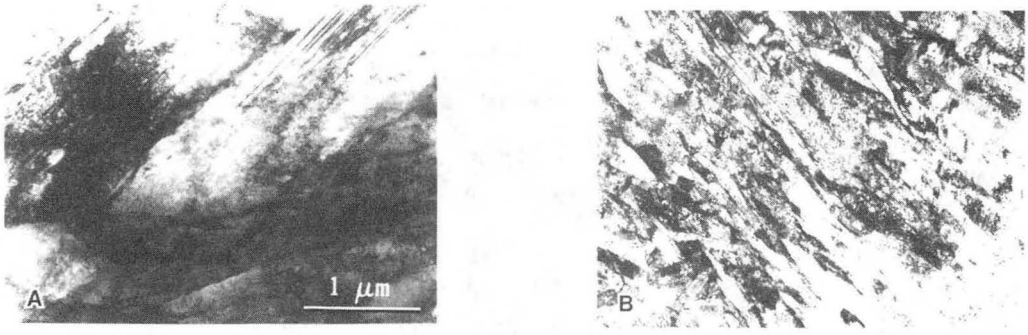

Fig 7. Bright field (BF) micrographs showing characteristic configurations of (a) twinned martensite in the as-quench structure of alloy B austenitized at 1200°C for 1 hr. and (b) lath martensite in the as-quenched structure of alloy controlled rolled at 1150°C and 850°C by 50% reduction each.

tempered martensites many workers have found evidence to suggest a transition carbide phase. Jack [10] first established the structure of the phase as h.c.p. and named it ε-carbide. He proposed the following orientation relationship between martensite and carbide to be $(001)_\alpha$ //$(0001)_\varepsilon$ and $(101)_\alpha$ //$(1011)_\varepsilon$ .The results of this study [Fig. 9] agrees with Jack's relationship and the $[211]_\alpha$ growing direction suggested by Murphy and Whiteman [11].

The presence of retained austenite between the martensite laths was observed in both alloys [Fig. 10]. Although the mechanisms for retention of the high temperature fcc austenite phase are not fully understood, generally, one would expect that fcc stabilizing elements should promote the retention of austenite. Thomas and Rao [12] have shown that in alloys whose bulk Ms and Mf temperatures are above room temperature, austenite can be retained at room temperature only in the presence of interstitial C, which is the strongest fcc stabilizer. Stabilization due to carbon may be caused by i) chemical stabilization, ii) thermal stabilization, and iii) mechanical stabilization. In these mechanisms, the redistribution of solute element, especially carbon, is important. Sarikaya et al., using field ion atom probe analysis [13], showed that carbon partitioning does occur between austenite and martensite and that high carbon levels exist at the interface. Such work underlies the importance of carbon on the interface mobility during the growth of the laths as suggested by Schoen et al. [14]. The careful modification of composition in this study does not significantly change the morphology or the amount of retained austenite found in the reference steel.

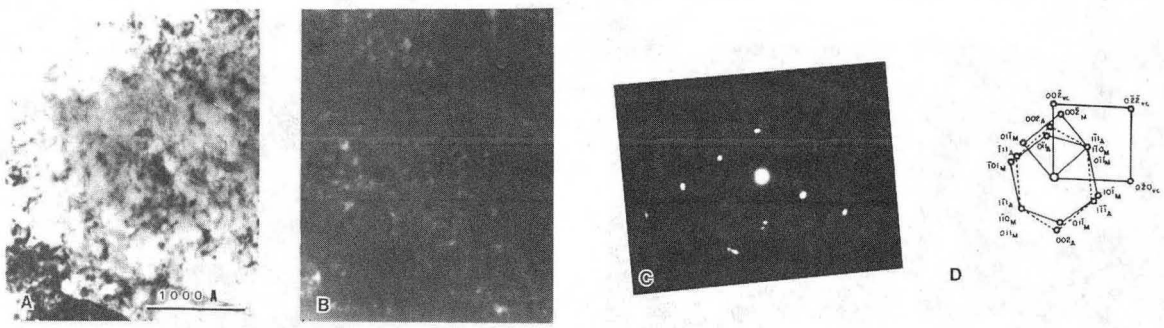

Fig 8.(a) BF, (b) DF of carbide 022 reflection (c) SAD pattern and (d) the corresponding indexed pattern of as-quenched structure of controlled rolled alloy B.The pattern corresponds to vanadium carbide VC.

XBB 845-3940

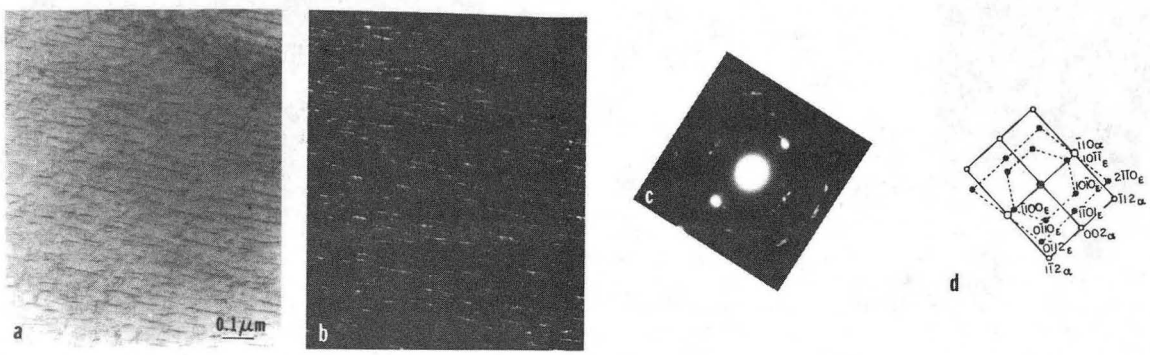

Fig 9.(a) BF, (b) DF image of $10\bar{1}0$ epsilon reflection (c) SAD pattern and (d) the corresponding indexed pattern of as-quenched structure of alloy A revealing the auto-tempered ε-carbide.

(iii) Tempered Structures

Tempering at 200°C does not change the as-quenched structure of alloy A significantly except for the precipitation of cementite (indicated by arrows in Fig. 11). The cementite platelets are about 200 Å wide and 0.2 μm long. The arrays of cementite are paralled to $\langle 111 \rangle_\alpha$ while those of ε-carbide are paralled to $\langle 211 \rangle_\alpha$ [Fig. 11]. The retained austenite is still stable at this tempering temperature. Fig. 12 shows the extensive amount of retained austenite as semi-continuous films in the 200°C tempered structure of alloy A.

The microstructures of alloy A tempered at 300°C were quite different from the microstructures of the as-quenched and 200°C tempered specimens. Extensive cementite precipitation or coarsening both inside the laths and at the lath boundaries were observed, as is well documented in the literature, e.g., ref. 15 and 16. The interlath cementite stringers at the lath boundaries are the products of the decomposition of retained austenite (tempered martensite embrittlement) [16]. The easy growth direction of the cementite is along the interfaces rather than into the martensite. As the carbon atoms diffuse into the newly formed cementite along the interfaces, there must be carbon depleted regions in the austenite. These regions then transform into ferrite, probably by a shear mechanism [13].

Fig. 13 shows the microstructure of alloy B thermally treated and tempered at 550°C for 1 hr. by carbon extraction replica and the results of EDX analysis on the carbide particles in the replica. It appears that there are, at least, two kinds of carbides, that is, chromium carbide which is

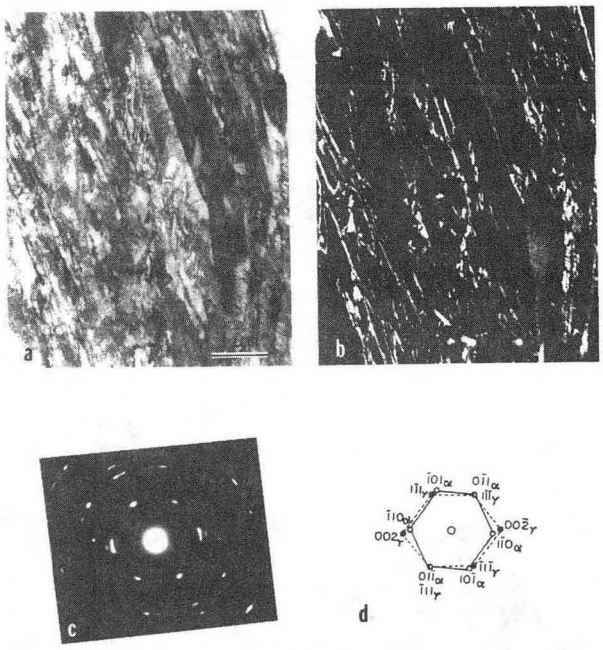

Fig 10. (a) BF, (b) DF of austenitic 002 reflection (c) SAD pattern (d)the corresponding indexed pattern of as-quenched structure of alloy A showing extensive films of retained austenite around martensite laths.

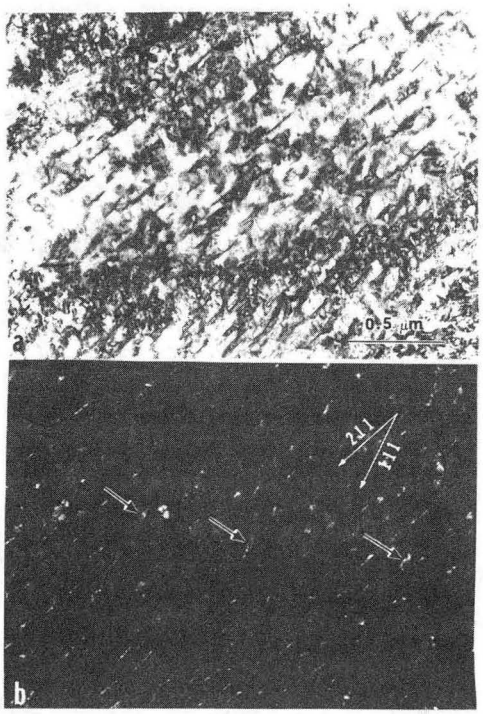

Fig 11. (a) and (b) DF of the 200°C tempered structure of alloy A revealing the ε-carbide and the cemenite together. Notice that the growing directions of (211 and 111) of the ε-carbide and the cementite are different.

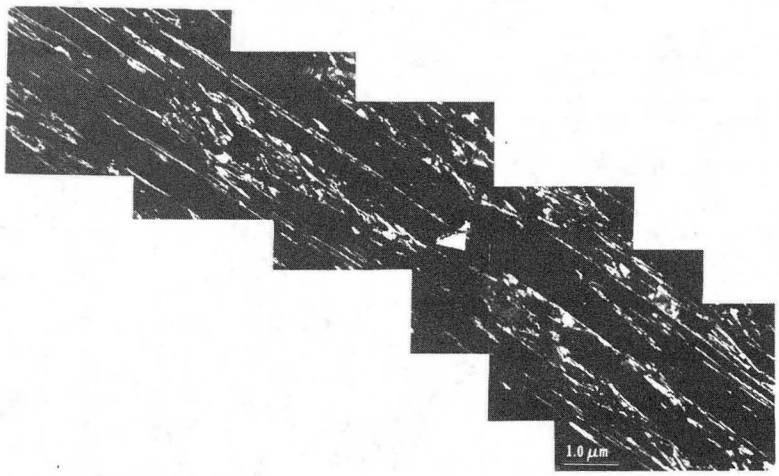

Fig 12. DF of the 200°C tempered structure of alloy A revealing extensive retained austenite films around martensite laths.

round and coarse and a complex carbide containing V which is fine and needle shaped. The latter carbides are responsible for the secondary hardening which offsets the softening due to tempering [Fig. 16]. Woodhead and Quarrel [23] reported that in a Fe/0.2C/1Mo/4.5Cr/1V steel, the stable carbides are M_6C, VC, and $CR_{23}C_6$, where M is a mixture of Mo,Cr,V and Fe. According to their results it could be deduced that the chromium carbide found in alloy B tempered at 550°C for 1 hr. might be $Cr_{23}C_6$ and the complex type of carbide might be M_6C, where M is a mixture of Mo,Cr,V and Fe.

B. Correlation of Mechanical Properties, Abrasion Resistance, and Microstructures.

The mechanical properties and the abrasion resistance of the alloy A designed in this study are summarized in Tables 2 and 3 and the values of alloys A,B are plotted as a function of tempering temperature in Figs. 14-17. Alloy A and thermally treated alloy B lose hardness rapidly in the tempering temperature range between room temperature and 400°C, whereas controlled rolled alloy B does not. The significant improvements in the impact toughness and the plane strain fracture toughness of alloy A upon 200°C tempering are associated with intra-lath precipitation of very fine carbides and increased stability of austenite films at the lath boundaries [16].

Abrasion resistance has been known to be directly proportional to the bulk hardness of annealed pure metals (e.g., 17,18) because hardness controls the penetration depth of the abrasives. The overall trends in the change of abrasion resistance and hardness with varying tempering temperature are very similar for the current work [Figs. 14,15]. However, the decreasing rate of abrasion resistance of alloy A upon 200°C tempering is lower than that of hardness. This may be explained in terms of toughness. The significant improvement of the toughness upon 200°C tempering seems to alleviate the decreasing rate of abrasion resistance, even though the hardness decreases rapidly. Upon 300°C tempering the hardness, and the toughness decrease drastically. The decrease of toughness is due to tempered martensite embrittlement as described in detail elsewhere [16] and the loss in hardness is typical of tempering due to growth and

coarsening of carbides. Comparing the hardness and the abrasion resistance of alloy A with those of thermally treated alloy B in the as-quenched to 400°C tempered conditions, the abrasion resistance of alloy A is higher than that of thermally treated alloy B while the hardness of alloy A is slightly lower than that of thermally treated alloy B. This indicates that dislocated lath martensite is superior to twinned martensite for abrasion resistance at the same hardness (strength) level. This supports the earlier work of Salesky et al. [19].

As the tempering temperature increases between 450°C~600°C, the hardness of thermally treated alloy B maintains the same level but the abrasion resistance slighly increases, whilst that of alloy A decreases continuously [Fig. 15]. In this temperature range fine alloy carbides form as shown by the extraction replica micrograph and x-ray microanalysis, Fig. 13. These alloy carbides are thermodynamically more stable than cementite and contribute to secondary hardening [20-22]. The maintenance of hardness and abrasion resistance of the thermally treated alloy B in this temperature range is attributed to the precipitation of these fine alloy carbides.

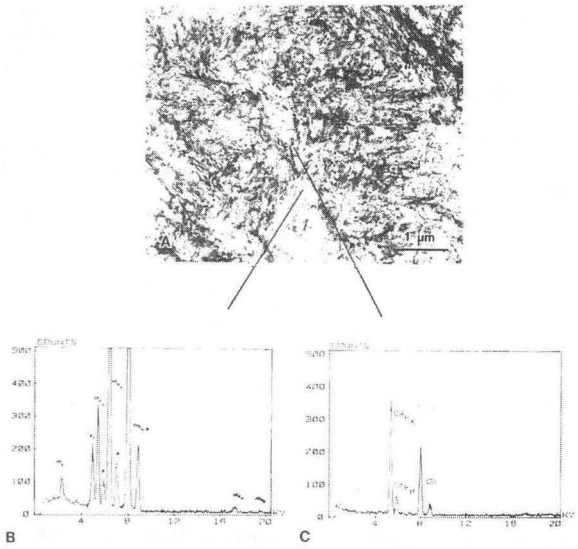

Fig 13. Carbon extraction replica of alloy B quenched from 1200°C and tempered at 550°C for 1 hr. and the results of EDX analysis on the carbide particles.

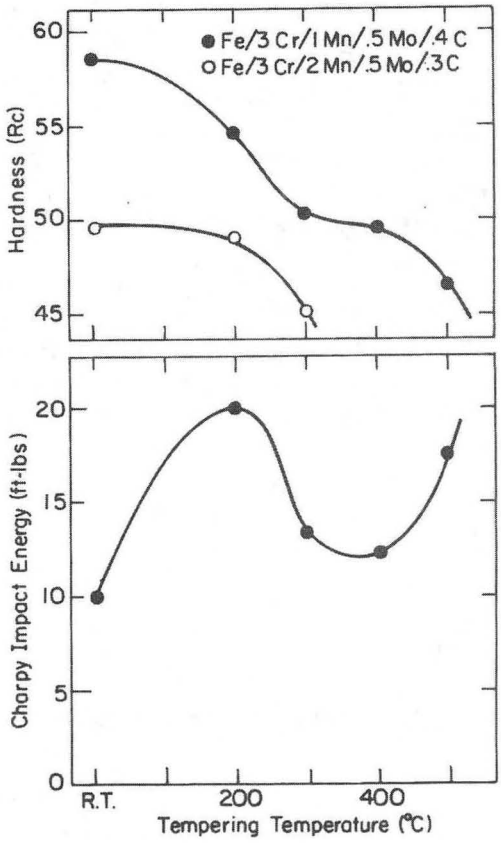

Fig 14. Hardness and Charpy impact energy vs. tempering temperature curves for alloy A. Data for Fe/3Cr/2Mn/0.5Mo/0.3C steel are from ref. 2.

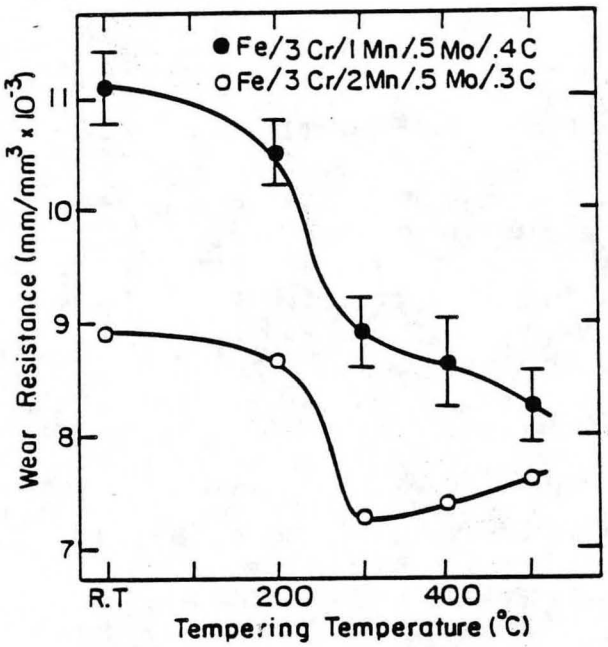

Fig 15. Wear resistance vs. tempering temperature curve for alloy A. Data for Fe/3Cr/2Mn/0.5Mo/0.3C steel are from ref. 24.

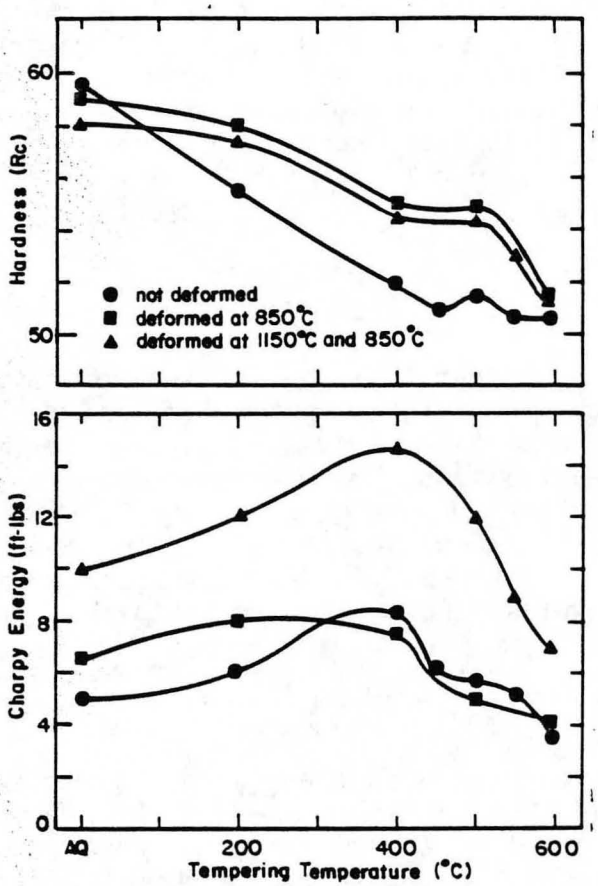

Fig 16. Hardness and Charpy Impact energy vs. tempering temperature curves for alloy B.

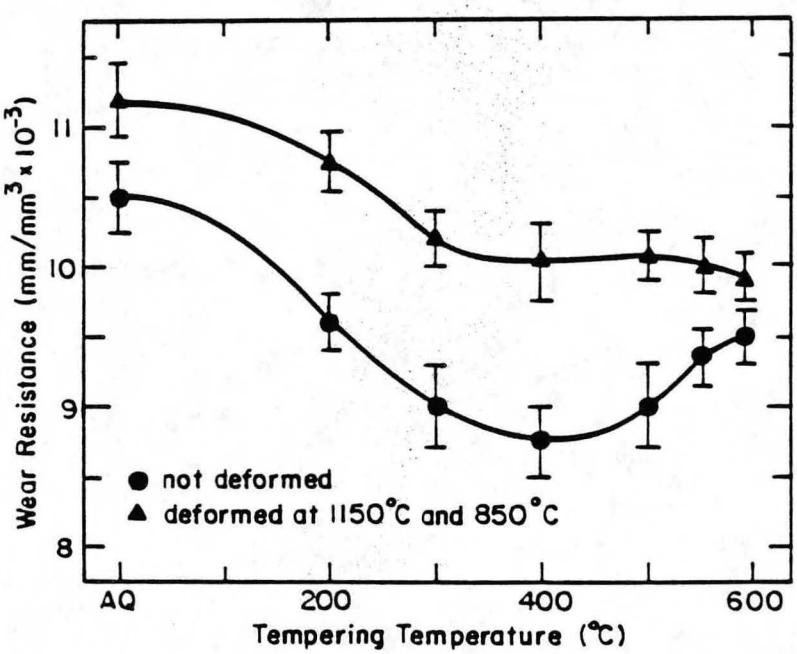

Fig 17. Wear resistance vs. tempering temperature curves for alloy B.

These alloy carbides are thus more effective than epsilon and iron carbide for improved wear resistance at high temperatures [Fig. 17]. For example, after tempering at 400°C, the abrasion resistance and impact toughness are improved 15% and 100%, respectively by controlled rolling of alloy B. The small grain size improves the impact toughness and precipitation of stable fine alloy carbides prior to martensite transformation [8] results in excellent tempering resistance.

SUMMARY

This work reaffirms the importance of grain size and martensitic microstructure (dislocated lath vs. twinned plates) on the strength and toughness of medium carbon steels, so that proper design of composition and processing leads to superior mechanical (Figs. 18,19) and wear (Fig. 20) properties. Controlled rolling is an effective method for grain size control without causing coarse carbides to develop. Microalloying with Mo and V is also helpful in contributing to secondary hardening and, thus improved strength and wear resistance at temperatures up to 500°C.

ACKNOWLEDGEMENTS

This work was supported by the Director, Office of Energy Research, Office of Basic Energy Sciences, Materials Science Division of the United States Department of Energy, under contract number DE-AC03-76SF00098. The alloys were supplied by Daido Steel Company, Japan.

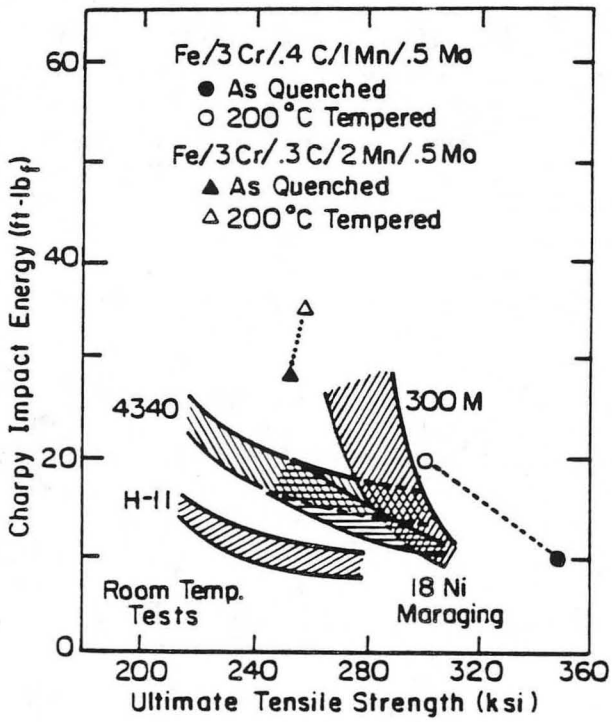

Fig 18. Fractographs of (a) 200°C tempered condition b) 300°C tempered condition for alloy A.

TABLE 2 Mechanical Properties of Alloy A

Tempering Temperature (°C)	Hardness (RC)	0.2 Pct Offset YS ksi	0.2 Pct Offset YS MPa	UTS ksi	UTS MPa	Pct Elongation Total	Pct Elongation (Uniform)	Kic ksi-in	Kic MPa-m	Charpy V-notch Energy ft-lb	Charpy V-notch Energy N-m
AQ	58.5	270	1860	350	2412	6.4	(3.0)	58.0	64.4	9.6	13.0
200	54.5	250	1723	300	2067	6.9	(3.3)	80.0	88.8	19.7	26.7
300	50.2	220	1516	255	1757	6.2	(2.9)	-	-	13.2	17.9
400	49.5	218	1502	250	1723	5.7	(2.7)	-	-	12.3	16.7
500	46.5	200	1378	225	1550	9.8	(3.1)	-	-	17.4	23.6
590	36.3	145	999	162	1116	15.0	(4.1)	-	-	65.4	88.7

TABLE 3 Wear Properties of Alloy A

Tempering Temp. (°C)	Weight Loss per One pass (mg)	Wear Resistance (mm/mm^3)
AQ	1.56	11100
200	1.64	10560
300	1.95	8880
400	2.03	8530
500	2.10	8250
590	2.2	7870

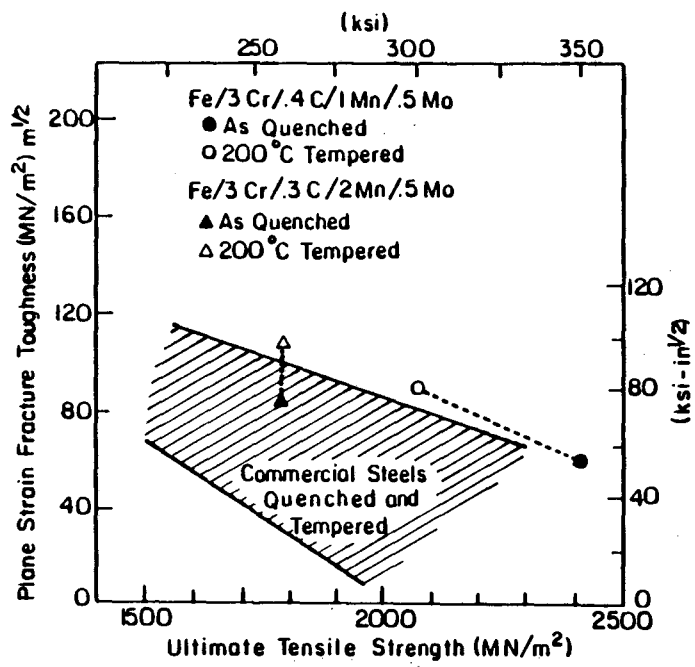

Fig 19. Comparison of toughness to strength relations in the experimental alloy A and equivalent commercial alloys. a) Charpy impact energy vs. tensile strength and (b) plane strain fracture toughness vs. tensile strength.

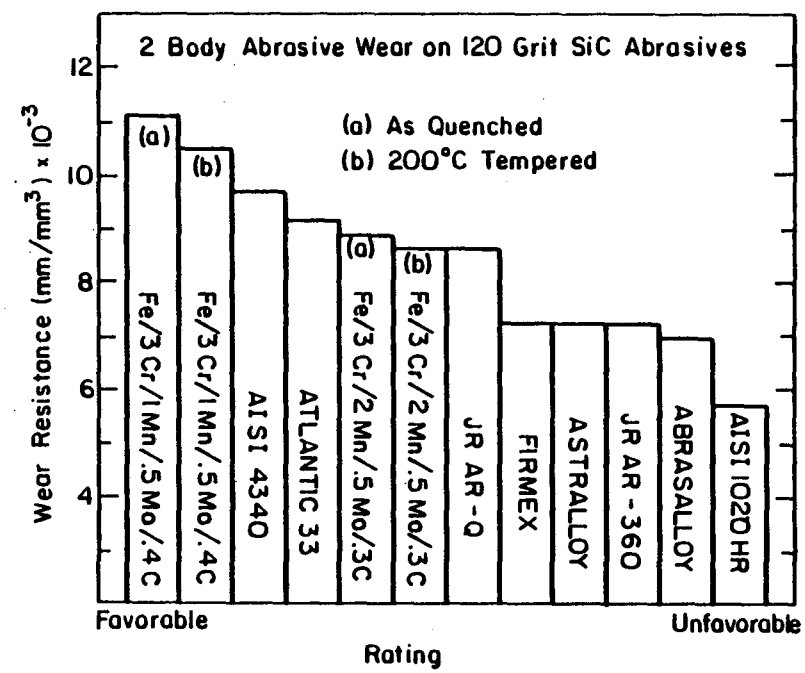

Fig 20. Comparison of wear resistance in the experimental alloy A and commercial abrasive or equivalent structural alloys. Data for commercial steels are from ref. 24.

REFERENCES

Pickering, F.B. 1978, Physical Metallurgy and Design of Steels. Applied Science Publishers LTD, London, p. 127.

Sarikaya, M., Steinberg, G.B., and Thomas, G. 1982 Met. Trans. 13A 2227.

Thomas, G. 1977, Fundamental Aspects of Structural Alloy Design. Ed. R. I. Jafee and B. A. Wilcox. Plenum Publishing, p 331

Thomas, G. 1973, Iron and Steel Int. 46 451.

Thomas, G. 1983, Specialty Steels and Hard Materials, Ed. N. R. Conrins and J. B. Clark. Pergamon Press, p 55

Phen, R. L., Lucklow, W.K., Mattson, L., Otth, D. and Tsou, P. 1977, Proc. Conf. on Coal Feeding Systems. JPL Publication, Pasadena, California 77-55 324

Johannson and Dandstrom, R. 1978, Mat. Science and Eng. 36 175.

Johari, O. and Thomas, G. 1965, Trans. ASM 58 563

Kwok, C. K. and Thomas, G. 1983, Wear of Materials, 140.

Jack, K. H., 1951, J. Iron St. Inst. 26 169

Murphy, S. and Whiteman, J. A., 1979 Met. Trans. 1 843

Thomas, G. and Rao, B.V N., 1978, Martensite Transformation, Academy of Science, Kiev, USSR, ICOMT 79 MIT Press p 12

Sarikaya, M., Thomas, G., Bernard, S.J., and Smith, G.D.W., 1982, Proc. Intl. Conf. on Solid Phase Transformations, Ed. H. I. Aaronson, D. E. Laughlin, R. F. Sekera, and C. M. Wayman, Warrendale, PA, pp 1421 and 999.

Schoen, F.J. and Owens, W.S. 1971, Met. Trans. 2 2431

Thomas, G. 1978, Met. Trans. 9A 439

Sarikaya, M., Jhingan, A.K., and Thomas, G. 1983, Met. Trans., 14A 1121

Khruschov, 1957, Prof. Conf. On Lubrication and Wear, Inst. of Mech. Eng., London, England, p 665

Richardson, R.C. 1968, Wear 11 245

Salesky, W.J., Fisher, R.M., Ritchie, R.O., and Thomas, G. 1983, Wear of Materials Book #H00254, Ed. K.C. Ludema, p 434

Payson, P. and Klein, J.L., 1943 Trans. ASM 31 218

Irvin, K.J. and Pickering, F.B. 1960, J. Iron St. Inst., 194 137

Honeycombe, R. 1972, Structure and Strength of Alloy Steels, Climax Molybdenum Co., Michigan

Woodhead, J. and Quarrel, A. 1966, The Role of Carbides in Low Alloy Creep Resisting Steels, Climax Molybdedum Co.

This report was done with support from the Department of Energy. Any conclusions or opinions expressed in this report represent solely those of the author(s) and not necessarily those of The Regents of the University of California, the Lawrence Berkeley Laboratory or the Department of Energy.

Reference to a company or product name does not imply approval or recommendation of the product by the University of California or the U.S. Department of Energy to the exclusion of others that may be suitable.

LAWRENCE BERKELEY LABORATORY
TECHNICAL INFORMATION DEPARTMENT
UNIVERSITY OF CALIFORNIA
BERKELEY, CALIFORNIA 94720